INFLUENCE OF LASER PULSE ENERGY ON VUV EMISSION FROM LASER PLASMAS UNDER VARIOUS AMBIENT CONDITIONS

MOHAMED A. KHATER

Department of Physics, College of Science, Al-Imam Mohammad Ibn Saud Islamic University (IMSIU), Riyadh, KSA, E-mail: drmakhater@gmail.com

Received September 23, 2011

The effect of laser pulse energy at different ambient atmospheres and pressures on the emission properties of laser-produced steel plasmas in the vacuum ultraviolet was investigated. For this aim, a time-integrated, space-resolved emission spectroscopic technique was developed. Air, argon and helium gases were used as the surrounding atmospheres, and pressures were varied from 0.005 mbar to 5.0 mbar depending on the gas composition. Fundamental (1.06 μm) pulses with energy between 200 and 800 mJ from a Q-switched Nd:YAG laser were employed to create the steel plasmas. At the highest pulse energy employed, *i.e.* 800 mJ, the best spectral line intensity was obtained in the argon atmosphere at a pressure of about 0.5 mbar. Moreover, it was found that at about 2.5 mm from the target surface the laser-plasma source produced the highest signal-to-background ratio using laser pulse energy of 400 mJ in air at about 0.1 mbar.

Key words: Laser-ablated plasmas, vacuum ultraviolet, spectral emission, laser energy, steel, LIBS.

1. INTRODUCTION

Laser-induced plasmas have proved to be useful spectroscopic sources for the direct elemental characterization of almost every type of material [1–8]. When the emitted radiation from the plasma is spectrally resolved, the parent species in the solid target are identified and quantified by their unique wavelengths and line intensities, respectively. The generic technique, usually termed *Laser Induced Plasma/Breakdown Spectroscopy* (LIPS or LIBS), is now well established. However, the interaction of pulsed, high-power lasers with solid materials and subsequent plasma generation are complex processes and strongly depend on several experimental parameters and conditions [9–15]. Accordingly, many studies have been carried out in order to optimize the experimental parameters involved in LIBS experiments and hence, improve the analytical performance of the technique. These parameters generally included the laser pulse characteristics (wavelength, energy, and duration) and focusing conditions, as well as the composition and pressure of various surrounding atmospheres [16–23].

For example, Sdorra and Niemax [18], using the fundamental radiation of a Nd:YAG laser with pulse energies between 2 and 20 mJ, recorded the emission intensities of analyte atoms as a function of the laser energy and buffer gas pressure in argon, neon, helium, air, and nitrogen. Kuzuya *et al.* [21] investigated the effects of laser energy and atmosphere on the emission characteristics of laser-induced plasmas with the use of a Q-switched Nd:YAG laser in the energy range between 20 and 95 mJ. Argon, helium, and air were used as surrounding atmospheres, and the pressures were changed from atmospheric pressure to 1 torr. More recently Sirven *et al.* [17] as well as Aguilera and Aragón [19] performed LIPS experiments on standard metallic samples, in air at atmospheric pressure, using a Nd:YAG laser at 1064 nm, with the aim of investigating the influence of laser pulse energy (varied between 5–23 mJ for the first group, and 20–100 mJ for the other group) on atomic emission properties.

However, all these studies were limited to LIBS employing spectral lines of neutral and/or singly charged species in the longer wavelength uv-visible region of the electromagnetic spectrum. Moreover, the laser energy values used were relatively low (2 to 100 mJ) and the pressures of background gases were restricted to relatively high values ranging between atmospheric pressure and approximately 5 mbar. Furthermore, these studies, and indeed almost all LIBS applications to date, have employed temporally resolved detectors to improve the spectral line contrast and so reduce the ultimate detection limit.

Khater *et al.* demonstrated an alternative approach that obviates the need for temporal resolution [8]. As the plasma spectral continuum emission takes place close to the sample surface, by using a simple spatial resolving mechanism to sample the emitted radiation from further-out regions of the plasma it is possible to enhance the spectral line contrast. When combined with deep vacuum ultraviolet spectroscopy to detect emission lines from ionic species, this time-integrated, spatially-resolved approach provides a competitive technique for the quantitative determination of carbon in steel alloys. In a subsequent publication [24], the same group carried out a comprehensive optimization study of different parameters and conditions for spatially resolved laser-induced plasma spectroscopy (LIBS) experiments in the vacuum ultraviolet (40–160 nm). The results demonstrated a set of optimum conditions for maximum spectral line intensities and signal-to-background ratios of laser-produced plasmas in the VUV regime and led to significantly improved carbon detection limits.

In the present work, we carry on our previous efforts by investigating the effect of laser pulse energy recorded at various ambient atmospheres (air, argon and helium) and pressures (0.005–5.0 mbar) on the emission characteristics of laser-ablated steel plasmas in the vacuum ultraviolet region. The remaining other conditions of the experiment were kept constant at the values previously obtained [24, 25] as shown in Table 1.

Table 1

Optimum base values of different experimental parameters and conditions employed in the present work

Experimental Parameter	Optimum Condition
Laser Wavelength	1.06μm (rep. rate 5.0 Hz)
Focusing Lens	Cylindrical; 2 mm defocused
Axial Distance	2.0–3.0 mm, from the target
Slit-Width	40 μm
Carbon Spectral Line	C(III) 97.70 nm

2. EXPERIMENTS AND DISCUSSION

A schematic representation of the experimental system is shown in Fig. 1.

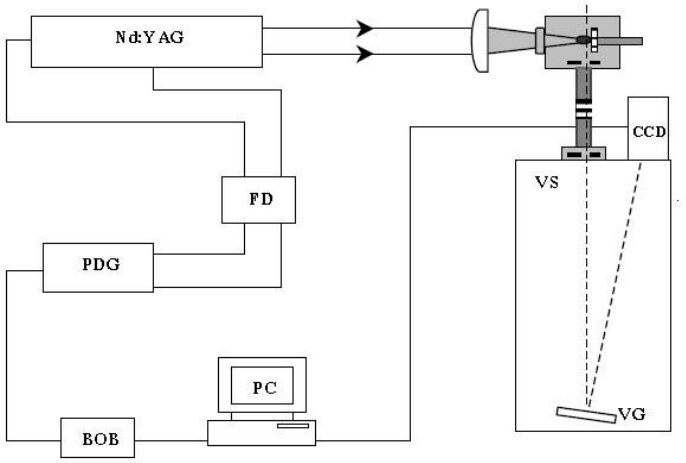

Fig. 1 – Schematic diagram of the experimental set-up. VS is vacuum spectrometer, VG is VUV grating, FD is frequency divider, PDG is pulse/delay generator and BOB is breakout box.

A detailed description of the setup used is fully depicted in previous publications [8, 24], and only a brief account of the equipment and procedures employed is given here. The plasma was generated by focusing high-powered, Q-switched Nd:YAG laser pulses (1.06 μm, 820 mJ max. energy and 7 ns pulse duration) onto the sample target surface within a vacuum-tight chamber. Throughout this work, a plano-convex cylindrical lens with nominal focal length of 150 mm was employed to focus the laser pulses. Accordingly, vertical line plasmas were formed at the target, whose length was about 8 mm which was approximately equivalent to the diameter of the incident laser-beam. The laser beam was focused 2 mm behind the target surface as this provided the best results in terms of emission intensities as well as signal-to-background ratios for the spectral line under investigation [9]. At this position, the groove width on the target was about

0.32 mm, corresponding to a power density of ~ 5.5 GW/cm^2. A vertical fore-slit, mounted inside the target chamber and positioned between the target and the entrance slit of the spectrometer, provided the necessary spatial discrimination in the plasma plume which expanded perpendicularly to the optical axis of the vacuum spectrometer. The fore-slit remained fixed in position while the target holder could be moved in the same direction as the plasma expansion, in order to spectrally access different spatial regions of the plume. Twenty laser shots were used to produce recorded emission spectra (ten additional pre-shots were fired on the target for cleaning purposes). A 1-m normal incidence vacuum spectrometer was used to disperse the light emitted from the plasma; the grating had 1200 lines/mm, and a reciprocal linear dispersion of 0.83 nm/mm in first order. The isolated radiation was recorded *via* a non gated VUV-sensitive, backside-illuminated and anti-reflection coated CCD array. The spectral resolution obtained from the combined spectrometer/CCD array system was valued at 0.045 nm in the first order. All measurements were carried out on a low alloy steel certified reference sample containing 0.91% carbon using the C(III) spectral line at 97.7 nm, as it proved to be the most sensitive carbon line in the VUV regime.

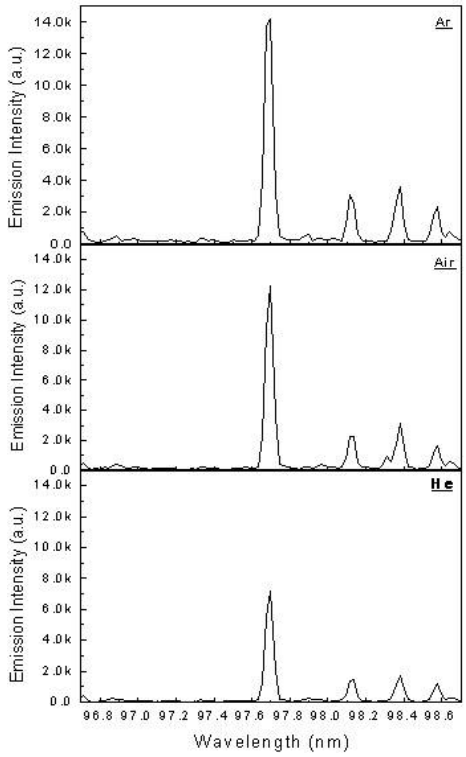

Fig. 2 – Part of laser-produced steel plasma emission spectra recorded at 2.5 mm with respect to the target surface, in helium at 0.5 mbar, air at 0.1 mbar and argon at 0.1 mbar for the C III 97.70 nm spectral; laser energy is 400 mJ.

All measurements were taken at the same fixed spatial position of 2.5 mm from the sample surface. This specific position was selected because, again, it provides the optimum emission characteristics for the CIII 97.7 nm in terms of intensity as well as signal-to-background ratio at intermediate pressure values [9]. At this intermediate location, temperate plasma confinement creates quite intense line emission with no corresponding excessive increasing in background continuum emission resulting in significantly improving their ratio.

Fig. 2 shows a part of laser-produced steel plasma emission spectra recorded at 2.5 mm with respect to the target surface, in helium at 0.5 mbar, air at 0.1 mbar and argon at 0.1 mbar for the C III 97.70 nm spectral line region. These conditions provided the highest signal-to-background ratios.

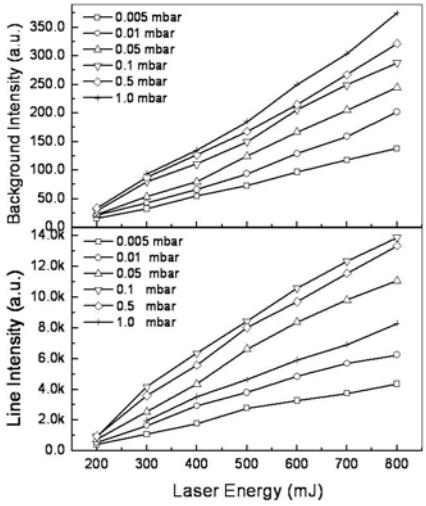

Fig. 3 – Influence of laser energy on spectral line as well as background emission intensities in air at different pressures.

The laser energy was varied from 200 to 800 mJ by simply changing the delay time between flash lamps and Q-switch onsets. The pressure of the ambient atmosphere was changed between 0.005 and 5.0 mbar, depending on the composition of the gas used. The flow rate of each gas was controlled by needle valves in the gas supply line, as well as in the pumping line [9]. Figures 3, 4 and 5 illustrates the dependence of the C(III) 97.70 nm spectral line intensity, as well as background intensity, on the laser pulse energy at different pressures of air, argon and helium atmospheres, respectively.

As can be seen from the figures, the spectral line as well as background emission intensities significantly increased with laser energy for all three atmospheres under consideration. The data points shown in the figures, which could also be fitted linearly, address some theoretical aspects of the laser-plasma

interaction phenomenon. For example, early during the incident laser pulse, the vapour formed in front of the target surface consists mainly of low electron and high neutral atom density. Absorption of laser photons in the plasma generally begins via electron-neutral *Inverse Bremsstrahlung* (IB). As the energy absorbed increases, the excitation temperature, T_{exc}, as well as ionization temperature, T_{ion}, increases and so too does the electron density of the plasma, n_e. As a result, the degree of ionization significantly enhances and the absorption of the laser beam by free-free electron transitions during collisions with positive ions becomes the dominant heating mechanism.

The highest emission intensities were produced in argon at a pressure of 0.5–1.0 mbar and for all laser energy values used. It should be noted at this stage that for each particular laser energy value, the spectral line intensity in both air and argon atmospheres showed a gradual increase with the pressure up to a certain value. Depending on the composition of the gas, this specific pressure was around 0.1 mbar in air and between 0.5 mbar and 1 mbar in argon. Raising the pressure beyond these values resulted in a significant reduction in the line emission intensities. This intensity decrease was much more pronounced in argon than in air atmosphere. In the case of helium, however, the line intensity kept increasing with pressure up to the maximum value employed in this experiment, *i.e.* 5.0 mbar [9].

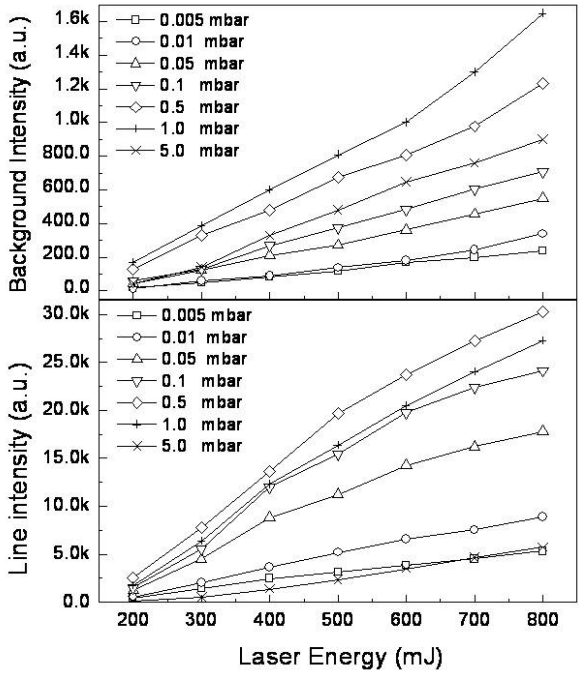

Fig. 4 – Influence of laser energy on spectral line as well as background emission intensities in argon at different pressures.

The significant enhancements in the spectral line intensities for air, argon, and helium atmospheres, seen in Figures 3–5, may be explained in terms of additional excitation/ionization processes of the ablated sample material, taking place in the buffer gas plasma formed in front of the target surface. If gas metastable energy states become significantly populated in the plasma environment, they can transfer large amounts of energy to the ablated atoms/ions not only sufficient for ionization, but also to produce considerably populated excited ionic levels, thus enhancing their corresponding transitions.

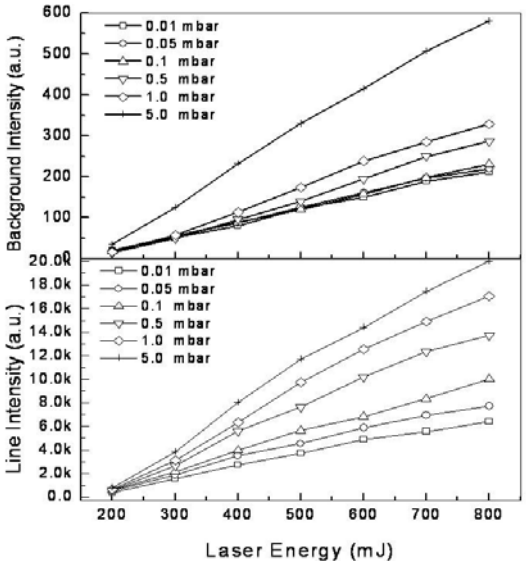

Fig. 5 – Influence of laser energy on spectral line as well as background emission intensities in helium at different pressures.

The efficiencies of atomization, excitation, and ionization processes in argon may be higher compared to air and helium atmospheres due to the fact that plasmas created in argon have higher electron temperatures [18], which was justified by higher emission intensities achieved. Furthermore, plasmas generated in argon have the highest electron densities compared to those produced in air or helium atmospheres as the heating of the gas plasma by inverse Bremsstrahlung (IB) mechanism is most effective if argon is used as the surrounding buffer gas. For laser ablation in vacuum, these important processes are absent and so the analytical efficiency is considerably lower.

The dramatic decrease in the spectral line intensities observed at higher pressures of air and argon atmospheres can be explained by the shielding effect [26]. Laser-induced argon breakdown plasmas can be formed in front of the solid target surface leading to a lowering of the laser-target coupling efficiency and a consequent reduction in the amount of material ablated from the sample. The

power density threshold required to induce a breakdown in the gas at those pressure values is usually on the order of 1×10^{12} W/cm^2; however, the presence of the solid target can significantly decrease the gas breakdown threshold and the probability of gas breakdown considerably increases, even at power densities on the order of 1×10^{6} W/cm^2 [1, 28]. Furthermore, due to the fact that the density of the ablation plasma produced under a high pressure ambient air and argon atmospheres is very high, the self-absorption of the spectral lines emitted within the "optically-thick" ablation plasma could be very important and leads to the apparent reduction in emission line intensities. This phenomenon is demonstrated in Fig. 6 by referring to the shape of the spectral lines emitted as the pressure of the argon gas increases.

Due to the higher ionization potential of helium compared to air and argon (24.6 eV for helium, 15.8 eV for argon, 15.6 eV for nitrogen, and 12.1 eV for oxygen), gas breakdown in helium does not take place, even at pressures ranging up to atmospheric, keeping the laser-target coupling efficiency high and leading to the intensity behavior seen.

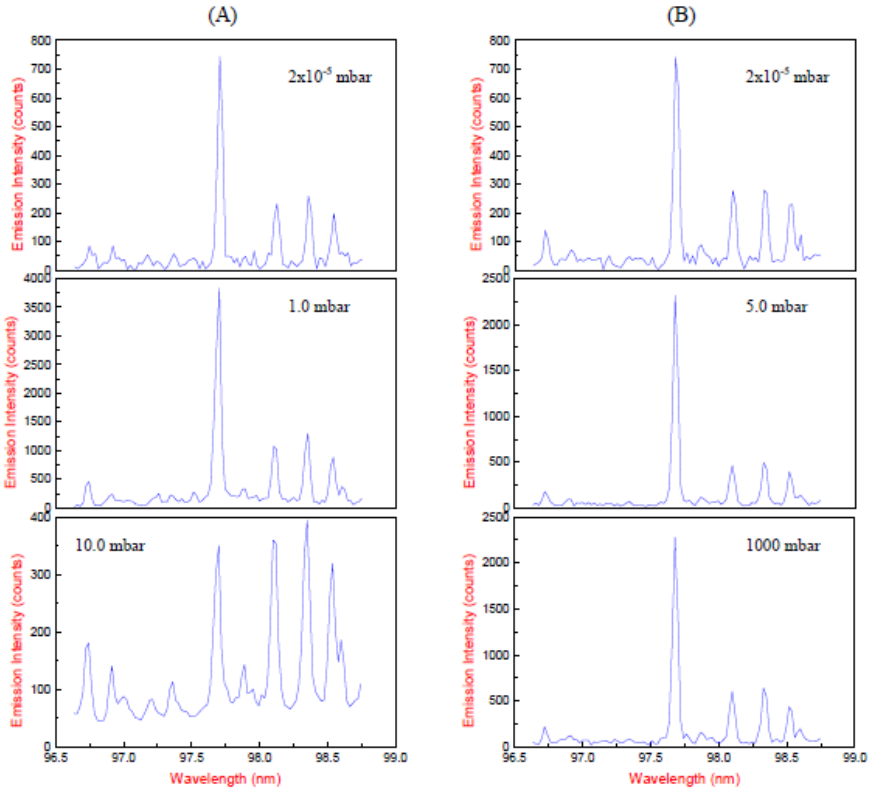

Fig. 6 – Spectra for the C III 97.70 nm line a different three pressures of Ar (A) and He (B) atmospheres.

To support the previous discussion, we present spectra of the CIII 97.7 nm spectral line for three selected pressures of both argon and helium gases in Fig. 6. Note that the middle spectrum in each figure represents the pressure value of either argon or helium atmosphere at which the emission intensity of the corresponding spectral line reached its highest value.

The above explanations are in a firm agreement with the experiments carried out by Iida [27], in which the amount vaporized from the solid target significantly decreased above a certain argon pressure (0.01–1 mbar) in comparison to that in the helium atmosphere. The condition necessary for the development of a cascade-like growth in the electron number density of laser-induced gas breakdown plasmas is given by the following formula [28]:

$$\frac{\mathrm{d}\varepsilon}{\mathrm{d}t} = \left(\frac{4\pi e^2 I \nu_{eff.}}{m_e c \omega^2} \right) - \left(\frac{2 m_e \nu_{eff.} \mathrm{E}}{M} \right) \rangle 0$$

where ε is the energy of the free electron with charge e and mass m_e, M is the mass of the neutral gas particles, E is the energy of the first ionization stage of the gas atoms, $\nu_{eff.}$ is the effective frequency of electron collisions with the gas particles, and I and ω are the laser power density and angular frequency, respectively. The first term in the equation expresses the rate of growth of the energy of free electrons as a result of the inverse Bremsstrahlung effect, while the second term represents the maximum rate of energy loss due to elastic collisions with the neutral particles of the gas.

In comparing argon and helium gases, the cascade condition expressed is more favored by argon (M = 40, and E = 15.8 eV) rather than helium (M = 4, and E = 24.6 eV). The result is that plasmas developed in an argon atmosphere are more absorptive than those in a helium atmosphere, due to their higher electron number densities and degree of ionization. Accordingly, the absorption of laser radiation by argon plasmas is more significant than in helium plasmas, and increases with pressure.

The background emission intensity, on the other hand, also monotonically increased with the laser energy for all three atmospheres used. The argon atmosphere produced the highest background intensities, while much smaller levels were obtained in air and helium, and they were approximately identical for a particular laser energy and pressure. Also, in the case of helium and at low pressures the background intensity is less sensitive to changes in laser energy than argon and air atmospheres. However, at higher pressures of helium the rate of increase in the background intensity is greater compared to the other two gases. Beyond 1 mbar pressure in argon, the background intensity dramatically decreased with laser energy. On the other hand, reduction of the background intensity with increasing the pressure of helium was not observed up to 5 mbar. The approximate similarities in the spectral emission characteristics of plasmas created in air and

argon atmospheres, compared to helium, in the pressure range studied can be described, to some extent, on the basis of differences in the mass density of the respective gas [21]. The density of helium is about one order of magnitude lower than that of argon, while the density difference between argon and air is very small.

Analytical capability is determined mainly by the line-to-background intensity ratio. The dependence of the signal-to-background ratios for the C III 97.70 nm spectral line on both the laser energy and pressure of the three atmospheres investigated is shown in Fig. 7.

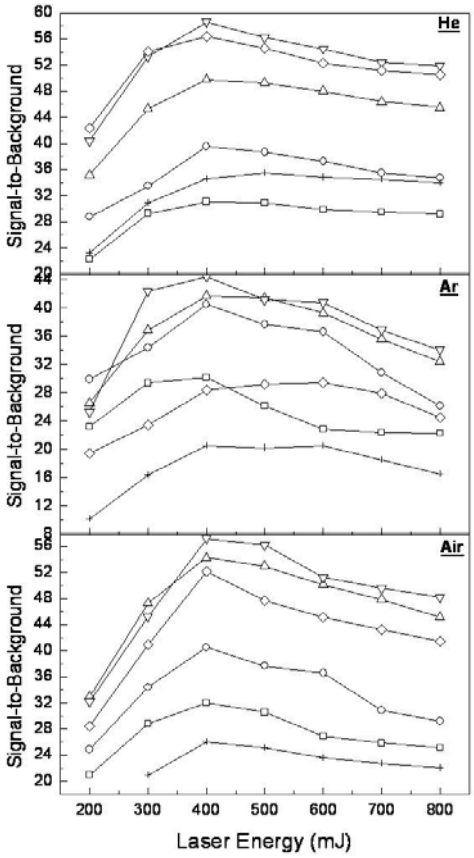

Fig. 7 – Signal-to-background ratios for the C III 97.70 nm spectral line as functions of laser energy at different pressures of the three atmospheres under study. See previous figures for definition of data symbols.

The data in the figure were derived from those obtained in Figures 3–5. For each atmosphere under study, signal-to-background ratios increased considerably with the laser energy and pressure. However, at a particular laser energy value of 400 mJ the signal-to-background ratios started a gradual decrease, the nature of

which strongly depends on the composition as well as pressure of the filled gas. This specific pressure valued at about 0.1 mbar in air and argon, and between 0.1 mbar and 1 mbar for helium. The signal-to-background ratios maximized at intermediate laser energy of 400 mJ, for all three atmospheres and at each particular pressure.

However, in the argon atmosphere the signal-to-background ratios leveled off at relatively higher pressures (0.5–1 mbar) in the energy range 400–600 mJ, before it slowly decreased for higher energy values. The same tendency was observed in the helium atmosphere at a pressure of 5 mbar. It is also seen from the figure that the highest signal-to-background ratios were obtained in both air and helium atmospheres, at relatively high pressures of 0.1 mbar and 0.5 mbar, respectively.

In approximately the center of the plasma (~ 2.5 mm from the target surface) and for each particular gas pressure, raising the laser pulse energy results in increasing the amount of ablated material that leads to enhancing the line emission intensity and hence signal-to-background ratios. Nevertheless, raising the laser pulse energy beyond a specific value leads to increasing the number of free electrons (electron number density is an increasing function of electron temperature) and hence enhancing the rate of various atomic processes responsible for emission of continuum background radiation [29–31].

3. CONCLUSION

The results confirm the strong dependence of plasma emission characteristics for the CIII 97.7 nm spectral line on the laser pulse energy. All measurements were recorded approximately in the center of the plasma ~ 2.5 mm from the target surface as it produced the optimum signal-to-background ratio of the line under investigation. Both line and background continuum intensities increase with the laser pulse energy up to the maximum value employed in this work, *i.e.* 800 mJ. On the other hand, the signal-to-background ratios monotonically increase up to specific laser pulse energy of 400 mJ, before they gradually decrease due to increase in the electron number density. In general, the emission characteristics of the vacuum ultraviolet-based carbon spectral lines were similar to those previously investigated in the uv-visible spectral range.

Acknowledgements. The author would like to acknowledge support from Enterprise Ireland under the Basic Research Programme scheme, Grant SC/1999/221, and the Higher Education Authority under the Programme for Research in Third Level Institution.

REFERENCES

1. S. A. Darke and J. F. Tyson, J. Anal. At. Spectrom. **8**, 145 (1993).
2. A. P. M. Michel, Spectrochim. Acta B **65**, 185 (2010).
3. J. J. Laserna *et al.*, Quim. Anal. (Barcelona) **15**, 45 (1996).

4. E. Tognoni *et al.*, Spectrochim. Acta B **65**, 1 (2010).
5. R. E. Russo, Appl. Spectrosc. **49**, 14A (1995).
6. R. Noll *et al.*, Spectrochim. Acta B **63**, 1159 (2008).
7. B. Bousquet *et al.*, Spectrochim. Acta B **63**, 1085 (2008).
8. M. A. Khater *et al.*, J. Phys. D: Appl. Phys. **33**, 2252 (2000).
9. B. C. Castle *et al.*, Appl. Spectrosc. **52**, 649 (1998).
10. W. Sdorra *et al.*, Mikrochim. Acta **108**, 1 (1992).
11. S. Darwiche *et al.*, Spectrochim. Acta Part B **65**, 738 (2010).
12. R. A. Multari *et al.*, Appl. Spectrosc. **50**, 1483 (1996).
13. L. St-Onge *et al.*, Spectrochim. Acta B **53**, 407 (1998).
14. Y. I. Lee and J. Sneddon, Spectrosc. Lett. **29**, 1157 (1996).
15. H. Kurniawan *et al.*, Appl. Spectrosc. **46**, 581 (1992).
16. Z.-W. Hwang *et al.*, Appl. Spectrosc. **45**, 435 (1991).
17. J. B. Sirven *et al.*, Spectrochim. Acta B **63**, 1077 (2008).
18. W. Sdorra and K. Niemax, Mikrochim. Acta **107**, 319 (1992).
19. J.A. Aguilera and C. Aragón, Spectrochim. Acta B **63**, 793 (2008).
20. J. Li *et al.*, Opt. Laser Techn. **41**, 907 (2009).
21. M. Kuzuya *et al.*, Appl. Spectrosc. **47**, 1659 (1993).
22. C. Barnett *et al.*, Spectrochim. Acta B **63**, 1016 (2008).
23. K. L. Eland *et al.*, Appl. Spectrosc. **55**, 279 (2001).
24. M. A. Khater *et al.*, Appl. Spectrosc. **56**, 970 (2002).
25. M. A. Khater, J. Korean Phys. Soc. **58(6)**, 1581 (2011).
26. Y. W. Kim, *Fundamentals of Analysis of Solids by Laser-Produced Plasmas*, in *Laser-Induced Plasmas and Applications*, Dekker, New York, 1989.
27. Y. Iida, Spectrochim. Acta Part B **45,** 1353 (1990).
28. G. W. Weyl, *Physics of Laser-Induced Breakdown: An Update*, Dekker, New York, 1989.
29. T. P. Hughes, *Plasmas and Laser Light*, Adam Hilger, UK, 1975.
30. G. Bekefi *et al.*, *Spectroscopic Diagnostics of Laser Plasmas, in Principles of Laser Plasmas* (Bekefi G, Ed.), John Wiley & Sons, Inc., 1976.
31. M. A. Khater and E. T. Kennedy, EPJ Plus **127(6)**, 61 (2012).